Food & Function

Impact of delivery system format on curcumin bioaccessibility: Nanocrystals, nanoemulsion droplets, and natural oil bodies

Journal:	*Food & Function*
Manuscript ID	FO-ART-12-2018-002510.R2
Article Type:	Paper
Date Submitted by the Author:	25-Apr-2019
Complete List of Authors:	Zheng, Bingjing ; University of Massachusetts, Food Science Zhang, Xiaoyun ; University of Massachusetts, Food Science Peng, Shengfeng; Nanchang University - Qingshanhu Campus North, State Key Laboratory of Food Science and Technology McClements, David; University of Massachusetts, Food Science

Impact of curcumin delivery system format on bioaccessibility: Nanocrystals, nanoemulsion droplets, and natural oil bodies

Bingjing Zheng[a], Xiaoyun Zhang[a], Shengfeng Peng[b], and David Julian McClements[a]

[a] Biopolymers and Colloids Laboratory, Department of Food Science, University of Massachusetts Amherst, Massachusetts 01003, United States

[b] State Key Laboratory of Food Science and Technology, Nanchang University, Nanchang, Jiangxi, China

Journal: Food and Function

Revision Submitted: April 2019

Corresponding author:

David Julian McClements, **E-mail address:** mcclements@foodsci.umass.edu; **Telephone:** +1413 545 2275

Abstract

Curcumin, a hydrophobic yellow-orange crystalline substance derived from plants, is claimed to exhibit a broad range of biological activities. Its application in functional foods and beverages is often limited by its low solubility in aqueous media, chemical instability, and low bioavailability. Previously, we have shown that curcumin can be successfully loaded into emulsions using the pH-shift method. In this study, we compared the efficacy of curcumin crystals dispersed in water (control) with three delivery systems produced using the pH-shift method: curcumin nanocrystals; curcumin-loaded nanoemulsions; and curcumin-loaded soy oil bodies. The nanoemulsions and oil bodies formed creamy yellow dispersions that were stable to creaming, whereas the nanocrystals formed a cloudy yellow-orange suspension that was prone to sedimentation. The gastrointestinal fate of the delivery systems was assessed using a static *in vitro* digestion model consisting of mouth, stomach, and small intestine phases. The nanoemulsions and oil bodies were rapidly and fully digested, while the nanocrystals were not. All three systems were relatively stable to chemical transformation in the *in vitro* digestion model. The nanocrystals gave a low bioaccessibility but the other two systems gave a high bioaccessibility, which was attributed to their ability to form mixed micelles to solubilize the curcumin. These results have important implications for the creation of more effective delivery systems for curcumin.

Keywords: curcumin; nanocrystals; soymilk; nanoemulsions; bioaccessibility; bioavailability; nutraceuticals.

1. Introduction

Turmeric is commonly used in Asian cuisine as a natural pigment and spice due to its distinctive yellow-orange color and unique flavor profile [1]. It has also been utilized for thousands of years as a therapeutic agent in traditional Chinese and Indian medicine [2, 3]. Curcumin is one of the principal bioactive compounds found in turmeric and is claimed to exhibit a range of health benefits, including the ability to prevent or treat cancer, depression, diabetes, obesity, pain, and stroke [4, 5]. Many researchers are now using the modern techniques and approaches of science and biomedicine to determine the molecular basis of its effects and to establish the veracity of these health claims. The results of mechanistic studies, mainly carried out in laboratories, suggest that curcumin does have antioxidant, anti-inflammatory, and antimicrobial properties, as well as modulating biochemical pathways that influence our health status [4, 6]. The findings from randomized clinical trials (RCTs), however, are inconclusive, with some suggesting that consumption of curcumin has beneficial effects and others not [7].

There are numerous challenges that food formulators face when trying to incorporate curcumin into functional foods and beverages, which are associated with its strong color, low water-solubility, poor chemical stability, and low bioavailability [8]. These same factors may also contribute to the inconsistent results obtained in clinical trials of curcumin's efficacy, since the solubility, stability, and bioavailability of curcumin are rarely measured or controlled in these studies [9]. Effective delivery systems are therefore needed to encapsulate and protect curcumin so that it can be successfully introduced into commercial foods and beverages in a bioactive form [10].

Many different kinds of curcumin delivery system have been developed, including micelles, nanoemulsions, emulsions, liposomes, biopolymer nanoparticles, microgels, and molecular complexes, which have been reviewed in detail elsewhere [10-13]. Each of these systems has its

own benefits and limitations for specific applications, which are influenced by numerous factors, including the ease of manufacture, cost, robustness, physicochemical properties, sensory attributes, loading capacity, and bioavailability [14]. Curcumin can be loaded into the particles present in colloidal delivery systems using a variety of methods. For instance, in the case of emulsions, curcumin can be dissolved into the oil phase before homogenization or incorporated into the oil droplets after homogenization. Recently, a simple low-cost method has been developed to load curcumin into preformed colloidal particles, which is based on the pH-dependence of its water-solubility [15]. Curcumin is non-charged at low pH values (< pH 8) and has a low water-solubility but it is negatively charged at higher pH values and so has a high water-solubility. The pH-shift method utilizes this phenomenon to load curcumin into the hydrophobic interiors of colloidal particles, such as casein micelles [15], biosurfactant micelles [16, 17], and emulsions [18]. Typically, the curcumin is dissolved in a strongly alkaline solution which is then mixed with an acidic colloidal dispersion. The reduction in the water-solubility of curcumin at lower pH values drives it into the hydrophobic interior of the colloidal particles.

Previously, we have demonstrated that curcumin can be successfully loaded into emulsions using a pH-shift method, and that the resulting system has good bioaccessibility as measured using an *in vitro* digestion model[18]. In the current study, we used the pH-shift method to create three different kinds of curcumin-loaded delivery systems: curcumin nanocrystals: curcumin-loaded oil bodies (soy milk); and curcumin-loaded nanoemulsions. The formation, physicochemical stability, and gastrointestinal fate of these delivery systems was then measured, as well as their impact on the bioaccessibility of the encapsulated curcumin. This study shows that the pH-shift approach is a simple and versatile method that can be used to load curcumin

into a variety of different colloidal delivery systems, including plant-based milks and nanoemulsions.

2. Material & Methods

2.1 Materials

Corn oil (Mazola, ACH Foods, Cordova, TN) and soymilk (Dairy-free Soy Creamer, Silk, Broomfield, CO) were purchased from a local supermarket and used without further purification. Curcumin (purity 95%) was obtained from Tokyo Chemistry Industries Company (Tokyo, Japan). The following chemicals were purchased from the Sigma-Aldrich Chemical Company (St. Louis, MO): mucin from porcine stomach (M2378-100G); pepsin from porcine gastric mucosa (P7000-25G); lipase from porcine pancreas pancreatin (P8096-100G); porcine bile extract (B8831-100G); sodium hydroxide (SS266-4L); sodium chloride (S640-3); ammonium nitrate (A9642-500G); potassium phosphate (P285-500); Nile Red (N3013-100MG); potassium citrate in basic monohydrate (P1722-100G); uric acid sodium salt (U2875-5G); urea (51456-500G); lactic acid sodium salt (71718-10G); and, hydrochloric acid (A144212-2.5L). Potassium chloride (P217-500G) and calcium chloride (C1016-500G) were purchased from Fisher Scientific (Fair Lawn, NJ). Quillaja saponin (Q-Naturale® 200) was provided by Ingredion Inc. (Westchester, IL). Chloroform and other reagents were all of analytical grade.

2.2 Preparation protocol

The pH-driven method was used to produce three different kinds of colloidal delivery system: curcumin nanocrystals; curcumin-loaded lipid droplets; and, curcumin-loaded oil bodies. This method required the use of a stock alkaline curcumin solution (6 mg/g), which was prepared by dissolving powdered curcumin into sodium hydroxide solution (0.1 N, pH 12.5) for 2 min in

the dark at room temperature. The behavior of the delivery systems was compared to that of a control, which consisted of curcumin powder dispersed directly into water. All systems were prepared so they had the same final curcumin concentration: 0.25 mg/g.

2.2.1 Control

The curcumin control was prepared by dispersing 7.5 mg of curcumin powder into 30 g of double distilled water and then stirring.

2.2.2 Curcumin nanocrystals

Suspensions of curcumin nanocrystals in water were prepared using the pH-driven method. The stock alkaline curcumin solution (6 mg/g) was diluted with double distilled water to reach a final concentration of 0.25 mg curcumin per g liquid. The resulting mixture was then immediately adjusted to pH 6.8 and stirred for 10 min in the dark at ambient temperature, which led to the spontaneous formation of curcumin nanocrystals.

2.2.3 Curcumin-loaded lipid droplets

Curcumin-loaded nanoemulsions were also prepared using the pH-driven method. The nanoemulsions used consisted of 10% (w/w) corn oil and 90% (w/w) aqueous emulsifier solution (2% Q-Naturale with 5 mM phosphate buffer solution, pH 6.8). Initially, a coarse emulsion was prepared using a high-shear mixer to blend the oil and aqueous phases together for 2 min (M122.1281-0, Biospec Products, Inc., ESGC, Switzerland). These systems were then passed five times through a high-pressure homogenizer (Microfluidizer M110Y, Microfluidics, Newton, MA) with a 75-μm interaction chamber (F20Y) at an operational pressure of 12,000 psi (83 MPa). The resulting nanoemulsions were then mixed with the stock alkaline curcumin solution and the mixture was immediately adjusted to pH 6.8 and stirred for 10 min in the dark at ambient

temperature. Double distilled water was used to dilute the curcumin-loaded nanoemulsions so the final system contained 5% oil and 0.25 mg of curcumin per g emulsion.

2.2.4 Curcumin-loaded oil bodies

Curcumin was loaded into commercial soymilk, which consists of soy oil bodies dispersed within a compositionally complex aqueous solution, using a similar protocol as used to load the nanoemulsions. A known amount of stock curcumin alkaline solution (1.25 g per 30 mL soymilk) was mixed with soymilk and then the mixture was immediately adjusted to pH 6.8. The resulting mixture was then stirred for 10 min in the dark at ambient temperature. The final system was diluted with double distilled water to reach a final concentration of 5% oil and 0.25 mg curcumin per g soymilk.

The composition of the soymilk reported on its label was: soymilk (filtered water, soybeans), cane sugar, palm oil, maltodextrin, contains 2% or less of soy lecithin, natural flavor, tapioca starch, locust bean gum, dipotassium phosphate.

2.3 Optical properties

The optical properties of the different systems were characterized using a colorimeter and digital camara. The instrumental colorimeter (ColorFlex EZ 45/0-LAV, Hunter Associates Laboratory Inc., Virginia, USA) was used to determine the color coordinates: L^* (darkness / lightness); a* (redness / greenness); and b^* (yellowness / blueness). A test sample (10 mL) was placed in a petri dish and illuminated with a D65-artificial daylight (10° standard angle) with a black background. The final values were obtained by averaging three replicate measurements per sample.

2.4 Simulated gastrointestinal tract model

153 A stimulated gastrointestinal tract (GIT), designed to mimic mouth, stomach, and small
154 intestine stages of the human gut, was used to analyze the potential gastrointestinal fate of the
155 curcumin-loaded delivery systems. An equal amount of each sample (30 mL), which contained
156 0.25 mg of curcumin per gram of sample, was transferred into a glass beaker for analysis. The
157 nanoemulsion and soymilk contained the same level of oil (5% w/w). This method was slightly
158 modified from the one used in our previous studies [19-21]

159 *2.4.1 Solution preparation*

160 For the oral phase, the artificial saliva stock solution (ASSS) and the stock simulated saliva
161 fluid (SSF) were prepared two days and one day before the study, respectively. The ASSS was
162 produced by dispersing sodium chloride (1.594 g/L), ammonium nitrate (0.328 g/L), potassium
163 phosphate (0.636 g/L), potassium chloride (0.202 g/L), potassium citrate (0.308 g/L), uric acid
164 sodium salt (0.021 g/L), urea (0.198 g/L), and lactic acid sodium salt (0.146 g/L) into double
165 distilled water (1 L) at 4°C overnight. A stock simulated saliva fluid (SSF) was prepared by
166 mixing 90 mg of mucin into 30 g of ASSS and storing the mixture at 4°C overnight before
167 carrying out the digestions.

168 For the gastric phase, a simulated gastric fluid (SGF) and simulated gastric fluid work
169 solution (SGFWS) were prepared. The SGF was prepared by fully dissolving sodium chloride (2
170 g/L) and hydrochloric acid (83.3 mM/L) into double distilled water at ambient temperature and
171 then stored at 4°C overnight before being used. The SGF was warmed to room temperature and
172 then the SGFWS was prepared by adding pepsin (3.2 mg/g) into the SGF with continuous
173 stirring for 30 min.

174 For the small intestinal phase, stock simulated intestinal fluids (SIF), bile salt solution, and
175 pancreatic lipase solution were prepared. The stock SIF was produced by dissolving calcium

chloride (5.5 g) and sodium chloride (32.87 g) in 150 ml in the double distilled water. The bile salt solution was prepared by continuously stirring porcine bile extract (53.57 mg/mL) with phosphate buffer (5 mM, pH 7) overnight at room temperature. Both stock solutions were stored at room temperature before being used. The lipase solution was prepared by mixing 0.9 mg of pancreatic lipase into 5 ml phosphate buffer (pH 7) immediately before adding to the sample.

2.4.2. GIT study

Curcumin-loaded samples were passed through stimulated mouth, stomach, and small intestine phases. To stimulate the mouth phase, the initial sample (30 mL) and SSF (30 mL) were preheated to 37 °C and transferred into a glass beaker. The mixture was adjusted to pH 6.8 and placed into a shaking incubator (Innova Incubator Shaker, Model 4080, New Brunswick Scientific, New Jersey, USA) with an operation of 100 rpm and 37 °C for 2 min. 40 ml of the "bolus" sample collected from the mouth phase was then mixed with preheated SGFWS (40 mL) and adjusted the pH to 2.5. The resulting mixture was agitated for 2 hours using the same incubator shaker. Finally, the "chyme" (60 mL) samples collected from the stomach phase were transferred to a fresh beaker and incubated in a water bath set at 37 °C. The pH of the sample was adjusted to neutral (pH 7.0) to create a small intestinal environment. Preheated SIF (3 mL) and bile salt solution (7 mL) were then added into the sample. The pH was adjusted back to neutral. Freshly prepared pancreatic lipase (5 mL) was then added to the mixture and the pH was again altered back to neutral. An automatic titration unit (Metrohm, USA Inc.) was used to monitor and maintain the sample at pH 7.0 by addition of sodium hydroxide solution (0.25 M). The volume of NaOH (V_{NaOH}) required to neutralize the solution was used to calculate the percentage of free fatty acids released:

$$FFA(\%) = 100 \times \frac{V_{NaOH} m_{NaOH} M_{lipid}}{2\, W_{liquid}}$$

Here, m_{NaOH} is the molarity of sodium hydroxide solution (0.25 M); M_{lipid} is the molecular weight of the oil used; and, W_{lipid} is the weight of the oil used in the digestion system (gram). This equation assumes that two fatty acids are released per triglyceride molecule if the reaction goes to completion.

2.5 Particle characterization

Two light scattering instruments were used to determine the particle characteristics during digestion. The mean particle diameter and particle size distribution were analyzed using a laser light scattering instrument (Mastersizer 2000, Malvern Instruments Ltd., Malvern, Worcestershire, U.K.). The ζ-potential values were determined using a particle electrophoresis device (Zetasizer Nano, Malvern Instruments, Worcestershire, U.K.). pH-adjusted double distilled water was used to dilute the samples collected from the mouth, stomach, and small intestinal phases, which had the same pH as the sample.

2.6 Microstructure analysis

The microstructure of the samples was characterized using light and confocal scanning fluorescence microscopy (Nikon D-Eclipse C1 80i, Nikon, Melville, NY, USA). The properties of the crystalline curcumin in the initial samples was determined using light microscopy with a cross-polarized lens (C1 Digital Eclipse, Nikon, Tokyo, Japan). Confocal scanning laser microscopy with a 200-fold magnification (20 × objective lens, 10× eyepiece lens) was used to determine the location of the oils and proteins in the samples. Nile red (1 mg/mL ethanol) and FITC (1mg/mL DMSO) dye solutions were used to stain the oils (red) and proteins (green) in the samples, respectively. The microstructure images were taken and analyzed using analysis software (NIS-Elements, Nikon, Melville, NY).

221 **2.7 Determination of curcumin concentration**

222 A UV-visible spectrophotometer (Cary 100 UV−Vis, Agilent Technologies, Santa Clara, CA,
223 USA) was used to determine the curcumin concentration in the initial samples, mixed micelle
224 fraction, and total digest fraction. An organic solvent, chloroform, was used to extract curcumin
225 from each sample by centrifuging at 3000 rpm for 10 min. The hydrophobic curcumin was
226 transferred into the chloroform layer. The curcumin concentration was then determined using
227 the UV-Vis spectrophotometer at a wavelength of 419 nm, and calculated based on a standard
228 curve prepared by measuring the absorbance of the known curcumin amounts (Supplementary
229 information Fig. 1).

230 *2.7.1. Encapsulation Efficiency*

231 The encapsulation efficiency of each delivery systems was determined using the following
232 expression:

233 $$\textit{Encapsulation Efficiency} = 100 \times C_{encapsulated} / C_{initial}$$

234 Here $C_{initial}$ and $C_{encapsulated}$ are the concentrations of curcumin initially added to the system and
235 that was encapsulated within the delivery system.

236 *2.7.2. Bioaccessibility and Stability*

237 After the small intestine phase, the samples were divided into two fractions: a micelle
238 sample and a total digest sample. The micelle sample was transferred into a centrifuge tube and
239 centrifuged (18,000 rpm, 25 °C) for 50 min (Thermo Scientific, Waltham, MA). The resulting
240 mixed micelle fraction was then collected as the clear supernatant of the samples. The total
241 digest sample and the initial sample were analyzed without any further processing. The
242 concentrations of curcumin in the mixed micelle ($C_{micelle}$) and total digest (C_{digest}) samples were
243 then measured using the spectrometry method described in Section 2.7. These values were then

used to calculate the *bioaccessibility* and *stability* of the curcumin-loaded samples. Here, $C_{micelle}$ represents the amount of curcumin solubilized within the hydrophobic interior of the micelles and vesicles formed in the small intestine, which is therefore in a form that is suitable for absorption. The value of C_{digest} represents the total amount of curcumin measured in the small intestine phase after digestion. The *bioaccessibility* was taken to be the percentage of curcumin solubilized in the small intestine that was solubilized within the mixed micelle phase, whereas the *stability* was taken to be the percentage of total curcumin that remained in the small intestine:

$$Bioaccessibility\ (\%) = 100\ \times \frac{C_{micelle}}{C_{digest}}$$

$$Stability(\%) = 100\ \times \frac{C_{digest}}{C_{initial}}$$

The stability therefore provides information about the potential degradation of curcumin within the simulated GIT.

2.8 Statistical analysis

Each experiment was repeated on at least three freshly prepared samples and the mean and standard deviation were calculated from these values. Statistical differences among samples were determined using statistical analysis software (SPSS, IBM Corporation, Armonk, NY, USA), and significant difference was considered to be $p < 0.05$.

3. Results & Discussion

3.1 properties of initial curcumin-containing food matrices

Initially, the pH-driven method was used to form curcumin nanocrystals, curcumin-loaded oil droplets, and curcumin-loaded oil bodies.

3.1.1 Encapsulation efficiency

The initial concentrations (C_I) of curcumin in the three samples produced using the pH-driven method were fairly similar to each other (Table 1), being around 230 μg/mL sample. The fact that the curcumin level in the samples was slightly less than the starting value (250 μg/mL) can be attributed to some curcumin degradation during sample preparation. Previous studies have reported that a small amount of curcumin is lost when it is solubilized in the strong alkaline solutions used in the pH-driven method [22, 23]. These values correspond to an encapsulation efficiency (EE) of around 93%, which is relatively high for colloidal delivery systems.

Overall, the pH-driven method was shown to be capable of successfully loading curcumin into both fabricated oil-in-water emulsions and commercial soymilk samples with a high encapsulation efficiency.

3.1.2 Curcumin structure and physical stability

The structure and location of the curcumin within the different samples were investigated using optical microscopy and digital photography (Fig. 1). The microscopy images showed that the control sample contained relatively large curcumin crystals (Fig. 1b), while the photographs showed that these crystals rapidly sedimented to the bottom of the test tubes (Fig. 1a). Presumably, this phenomenon occurred because the curcumin crystals were relatively large and denser than water. Consequently, they were particularly prone to gravitational separation in the form of sedimentation.

As expected, the curcumin nanocrystals formed by mixing the alkaline curcumin solution with water were much smaller than the curcumin crystals in the control (Fig. 1b), highlighting the ability of the pH-driven method to generate minute nutraceutical crystals. The nanocrystals appeared to have thin needle-like structures that tended to associate with each other, probably

because of hydrophobic attraction. The curcumin nanoparticle suspensions were relatively stable to gravitational separation immediately after fabrication (Fig 1a), forming a cloudy dispersion with a relatively uniform appearance. Even so, when they were allowed to stand for 2 hours an orange sediment was observed at the bottom of the test tubes (Fig. 1a), suggesting that sedimentation still occurred, albeit at a slower rate than for the control. This phenomenon can be attributed to the weaker gravitational forces acting on the nanocrystals.

Both the curcumin-loaded nanoemulsion and soymilk formed creamy yellow-orange dispersions with a uniform appearance, indicating that the oil droplets and oil bodies were stable to gravitational separation. No curcumin crystals were seen at the bottom of the test tubes or in the optical microscopy images when these samples were observed by visual inspection and optical microscopy (Figs. 1a and 1b). These results suggest that the pH-driven method was successful in loading the curcumin into the hydrophobic interiors of the lipid droplets and oil bodies.

3.1.3 Color coordinates

The color of the samples was quantified against a black background using an instrumental colorimetry (**Table 1**). Here, L^* is the light/dark axis, which varies from pure black (0) to pure white (100); a^* is the red-green axis, which varies from strongly red (positive) to strongly green (negative); and, b^* is the yellow-blue axis, which varies from strongly yellow (positive) to strongly blue (negative).

After stirring, the control, which consisted of curcumin powder dispersed in water, had a low lightness (L^*= +6.64), a moderate yellowness (b^*= +7.2) and a slight redness (a^*= +2.96) (Table 1). These color parameters can be attributed to the yellow-orange color brought by the curcumin crystals. The suspension of curcumin nanocrystals had a higher lightness (L^*= +25.81)

and yellowness (b^*= +38.80) than the control, and had a slight greenness (a^*= -2.62) rather than redness (Table 1). This effect can be attributed to the fact that the curcumin crystals were much smaller in this sample and so they scattered light more strongly and at different wavelengths [24]. As a result, more light was reflected from the surface of the samples, leading to a higher lightness. Moreover, the scattered light encountered a higher number of curcumin crystals and so there was a greater degree of selective absorption of the light waves, leading to a more intense yellow color and a change from reddish to greenish.

Interestingly, the curcumin-loaded nanoemulsions and oil bodies prepared using the pH-driven method had very similar color coordinates (Table 1). They both had relatively high L^* values, strongly positive b^* values, and slightly negative a^* values, which suggests they had a bright yellow color with a tinge of green. These effects can be attributed to the ability of the lipid droplets and oil bodies to scatter light waves strongly, as well as to the ability of the dissolved curcumin molecules to selectively absorb light waves [24, 25].

3.1.4 Particle characteristics

It was not possible to determine the characteristics of the particles in the samples containing curcumin crystals using light scattering because they were highly non-spherical, having a needle-like structure. One of the assumptions in the analysis of the data for both static and dynamic light scattering instruments is that the particles are spherical. For this reason, only the particle characteristics of the curcumin-loaded lipid droplets and oil bodies were measured.

The static light scattering measurements indicated that the nanoemulsions had a monomodal particle size distribution (PSD) and contained small lipid droplets, *i.e.,* $d_{32} < 200$ nm (Table 1 and Fig. 2). This indicates that the combination of emulsifier and microfluidizer used to prepare the nanoemulsions was effective at generating small lipid droplets. The oil bodies in the soymilk

had a bimodal PSD and contained somewhat larger particles (d_{32} > 400 nm) than those found in the nanoemulsions. The relatively large particles found in this commercial product are probably because the size of the oil bodies is determined by their natural origin, rather than homogenization. The broad particle size distribution may also have been because the soymilk contains a range of different types of colloidal particles and biopolymers, which could all have contributed to the light scattering signal.

As mentioned earlier, both the lipid droplets and oil bodies exhibited good stability against gravitational separation during storage. According to Stokes's Law, the velocity that a spherical particle moves through a fluid decreases as the particle size decreases, the fluid viscosity increases, and the density contrast decreases [26, 27]. The primary reason that the curcumin-loaded nanoemulsions were stable to creaming is the small size of the lipid droplets then contain. Conversely, the good stability of the curcumin-loaded the soymilk may have been because of the fairly small size of the oil bodies, as well as the increase in viscosity associated with the tapioca starch and locust bean gum used as thickening agents in this product.

The surface potential of the lipid droplets in the nanoemulsions (ζ = -55.8 mV) and the oil bodies in the soymilk (ζ = -30 mV) were both strongly negative (Table 1). A high surface potential is important for inhibiting particle aggregation in colloidal dispersions since it leads to a strong electrostatic repulsion [26, 27]. The high negative charge on the lipid droplets in the nanoemulsions was attributed to the fact that they were coated with a layer of quillaja saponins, which are known to be strongly anionic due to the presence of carboxylic acid groups on their surfaces. The high negative charge on the oil bodies in the soymilk may have been due to the fact that they are naturally coated by a layer of phospholipids and proteins that are anionic at neutral pH [28, 29].

The microstructure images of the nanoemulsion and soymilk further demonstrated the good aggregation stability of the lipid droplets and oil bodies (Figs.1 b and 5). Both confocal fluorescence and light microscopy images of the curcumin-loaded colloidal systems indicated that no aggregation occurred. However, the soymilk was seen to contain particles that had a broad range of sizes (Fig 1.b), which agrees with the PSD measurements. The wide range of particles in the soymilk may have been because of the natural variation in oil body dimensions [30] or because it contained a range of other types of colloidal particles and biopolymers, such as starch and locust bean gum.

3.2 Gastrointestinal fate of delivery systems

The curcumin-loaded nanoemulsion and soymilk samples were sequentially passed through artificial mouth, stomach, and small intestinal fluids to simulate passage through the human gut. Changes in the structural and physical properties of the samples were measured after exposure to each gastrointestinal stage. The two samples containing curcumin crystals dispersed in water, namely the control and nanocrystal samples, were not analyzed in these experiments because of difficulties in reliably characterizing their properties using light scattering techniques.

3.2.1. Influence of the GIT on particle properties

Oral phase: After exposure to the oral phase, there was a small but significant increase in the mean diameter of the particles in the nanoemulsions (Figs. 2 and 3). In addition, the magnitude of their negative charged decreased appreciably (Fig. 4). On the other hand, there appeared to be little change in the structural organization of the lipid droplets in the confocal microscopy images (Fig. 5). These results suggest that there was a small amount of lipid droplet aggregation under simulated oral conditions, which can be attributed to depletion or bridging flocculation caused by the mucin in the artificial saliva [31, 32]. In addition, there may have been

379 some electrostatic screening of the surface charge by electrolytes in the artificial saliva. In
380 contrast, there was little change in the mean particle size or surface potential of the oil bodies in
381 the soymilk after exposure to the simulated oral phase (Figs. 2 to 4). This suggests that the oil
382 bodies may have been more resistant to aggregation in the artificial saliva, possibly because the
383 mucin interacted with their surfaces less strongly [32-34]. The confocal fluorescence microscopy
384 images suggest that there may have been a small amount of clumping of the oil bodies in the oral
385 phase (Fig. 5), but presumably the flocs formed were so weak that they were easily disrupted
386 when the samples were diluted for the light scattering measurements.
387 *Stomach phase*: The nanoemulsions and soymilk behaved very differently under simulated
388 gastric conditions. There was no significant change in the mean particle diameter of the
389 nanoemulsions when they moved from the oral to stomach phase but a huge increase in the size
390 of the particles in the soymilk (Fig. 3). The PSD measurements and confocal fluorescence
391 images indicated that there was only a small amount of lipid droplet aggregation in the
392 nanoemulsions but extensive clumping of the oil bodies in the soymilk (Figs. 2 and 5).
393 The surface potential of the particles in both the nanoemulsions and soymilk were close to
394 zero after exposure to the small intestine conditions (Fig. 4). This effect can be attributed to a
395 number of physicochemical phenomena occurring in the stomach phase. First, any carboxylic
396 acid and amino groups on the saponins, phospholipids, and proteins would have become
397 protonated in the highly acidic environment of the gastric fluids, leading to a reduction in
398 negative charge and increase in positive charge. Second, the electrolytes in the gastric fluids
399 would have reduced the magnitude of the surface potential by screening the electrostatic
400 interactions. Third, the anionic mucin molecules arising from the artificial saliva may have
401 bound to cationic patches on the surfaces of the particles.

The extensive aggregation of the oil bodies in the soymilk observed under gastric conditions may have been because the soy proteins on their surfaces became positively charged, thereby promoting bridging flocculation by anionic mucin molecules in the surrounding aqueous fluids. Moreover, there would have been little electrostatic repulsion between the oil bodies because of their very low surface charge. Hence, the oil bodies may also have aggregated due to the van der Waals and hydrophobic attraction between them [35, 36]. In addition, the proteases (pepsin) in the gastric fluids may have hydrolyzed the proteins at the surfaces of the oil bodies, thereby reducing their aggregation stability [20]. Interestingly, the saponin-coated lipid droplets in the nanoemulsions were relatively stable to aggregation in the gastric fluids (Figs. 2, 3 and 5) even though they only had a very low surface potential (Fig. 4). This suggests that the saponin molecules formed a coating around the lipid droplets that was resistant to disruption in the gastric fluids. Furthermore, this coating may have inhibited extensive aggregation because it generated a strong steric repulsion between the droplets. The good gastric stability of saponin-coated lipid droplets has also been reported in previous studies [37, 38].

Small intestine phase: After incubation in the artificial intestinal fluids, the particles in the nanoemulsions remained relatively small (Figs. 2, 3 and 5). On the other hand, most of the large aggregates observed in the stomach phase broke down when the soymilk was incubated in the intestinal fluids. After exposure to lipase, there is likely to be many different kinds of colloidal particles present in the digest, including micelles, vesicles, calcium soaps, and undigested macronutrients, which all contribute to the light scattering signals used to measure the particle size and charge. The confocal microscopy images also showed that both samples contained a wide range of different sized particles.

The particles in the digests arising from the nanoemulsions (-68 mV) and the soymilk (-49 mV) had a strong negative charge. This effect can be attributed to the fact that many of the constituents in the digestion are anionic at neutral pH, including the bile acids, free fatty acids, saponins, and peptides.

3.2.2. Lipid digestion profiles

The digestion of the components in the different delivery systems was measured during incubation in the small intestine phase using a pH-stat automatic titration unit (Fig. 6). The volume of NaOH solution that had to be added to maintain a neutral pH within the reaction chamber was highly dependent on sample type. There was little change for both samples containing only curcumin crystals dispersed in water (control and nanocrystals), which should be expected because they did not contain any digestible materials. Conversely, there was a rapid increase in the volume of NaOH solution added to the nanoemulsion and soymilk samples during digestion, which suggests that the lipids in these samples had been easily digested by the lipase. Presumably, the lipase molecules adsorbed to the surfaces of the lipids droplets or oil bodies and hydrolyzed the triglycerides inside.

The percentage of free fatty acids (FFAs) released from these systems was calculated from the titration data (Fig. 6). These results show that the lipid phase was rapidly digested within the first 20 minutes of incubation in the small intestine phase, with slower digestion occurring at later times. By the end of the small intestine phase, most of the lipids in the nanoemulsions (> 86%) and soymilk (> 84%) had been digested. This finding can be attributed to the relatively small particle diameter of these colloidal systems, which leads to a large oil-water surface area for the digestive enzymes to attach and hydrolyze the triglycerides [39, 40]. These results suggest

446 that the small triglyceride particles in both the nanoemulsions and soymilk were easily accessible
447 to the lipase and effectively hydrolyzed.

448 **3.3. Bioaccessibility and transformation of curcumin in different delivery systems**

449 Finally, the curcumin concentration in the mixed micelles and in the total digest collected at
450 the end of the small intestine phase was measured for the various samples, and then the stability
451 and bioaccessibility of the curcumin was determined (Fig. 7). This information is important
452 because curcumin in a hydrophobic nutraceutical with a low water-solubility and poor chemical
453 stability. The concentration of curcumin in the total digest represents the fraction that survived
454 throughout the entire simulated GIT model. The concentration of curcumin in the mixed micelles
455 provides an indication of the fraction available for uptake by the epithelium cells.

456 The level of curcumin in the total digest was significantly lower for the control samples than
457 for any of the other samples (Fig 7a). This was probably because some of the large crystals in
458 the curcumin did not make it to the reaction chamber because they stuck to the side of the
459 containers or remained at the bottom of the samples. One would have expected the curcumin to
460 be most chemically stable in the large crystals in the control sample because they have the lowest
461 surface area exposed to water. There was no significant difference in the levels of curcumin in
462 the total digest for the nanocrystals, nanoemulsions, or soymilk (Fig. 7a), suggesting they all had
463 a similar effectiveness at protecting curcumin from chemical degradation. Nevertheless, there
464 was still a reduction in the total level of curcumin present in these samples compared to the
465 amount added initially, with only about 71%-75% remaining (Fig. 7b). This suggests that there
466 may have been some chemical degradation of the curcumin during its passage through the
467 simulated human gut. Curcumin is known to be highly unstable to degradation under neutral and

basic conditions, so it is possible that some transformation of the curcumin molecules occurred during incubation in the simulated mouth and small intestine conditions.

The bioaccessibility was calculated from the ratio of curcumin in the mixed micelle phase to the total digest (Fig. 7b). The bioaccessibility of the curcumin was much higher in the nanoemulsions and soymilk than in the nanocrystal dispersions. This effect can be partly attributed to the fact that the free fatty acids and monoglycerides generated during lipid digestion combined with the phospholipids and bile salts in the small intestinal fluids to form mixed micelles with a higher solubilization capacity for curcumin. Moreover, the transfer of curcumin molecules from the colloidal particles into the micelles may have been easier when they were solubilized in the hydrophobic interiors of the lipid droplets and oil bodies than when they were present in a crystalline form. Interestingly, the bioaccessibility of the curcumin was slightly higher in the soymilk than in the nanoemulsions (Fig. 7b). This suggests that the transfer of the curcumin molecules from the oil bodies to the mixed micelles may have been easier than from the saponin-coated oil droplets.

It should be noted that the commercial soy milk was reported to contain some lecithin and palm oil on its ingredient list. These ingredients might also have contributed to the bioaccessibility of curcumin measured for the soymilk. For instance, the phospholipids in the lecithin, as well as free fatty acids and monoglycerides resulting from digestion of the palm oil, could lead to the formation of more mixed micelles. In future studies, it would be useful to utilize pure oil bodies to investigate their encapsulation efficiency so as to avoid this effect.

4. Conclusions

In conclusion, this study demonstrated the effectiveness of the pH-driven method to load curcumin into the lipid droplets in nanoemulsions as well as the oil bodies in commercial

491 soymilks. Moreover, it showed that the pH-driven method could also be used to form curcumin
492 nanocrystals dispersed in water. The pH-driven method there appears to be a versatile tool for
493 creating different kinds of curcumin delivery systems.

494 The curcumin-loaded nanoemulsion and soymilk had a homogeneous appearance and good
495 stability to aggregation, which was attributed to the strong negative charge on the lipid droplets
496 and oil bodies. Moreover, the curcumin appeared to remain solubilized within the hydrophobic
497 domains of the lipid droplets and oil bodies, without any evidence of curcumin crystals being
498 formed. There were appreciable differences in the behavior of the nanoemulsions and soymilk in
499 the simulated GIT. In particular, the nanoemulsions appeared to be more susceptible to
500 aggregation in the mouth phase, whereas the soymilk was much more susceptible to aggregation
501 in the stomach phase. Nevertheless, both systems led to a relatively high stability and
502 bioaccessibility of the curcumin at the end of the small GIT model. In contrast, the curcumin
503 nanocrystals had a relatively low bioaccessibility because there were fewer mixed micelles to
504 solubilize the curcumin molecules.

505 Overall, our results show that curcumin can be loaded into different kinds of colloidal
506 delivery system using the pH-driven method and that these systems can have a high
507 bioaccessibility. Consequently, the nanoemulsions and plant-based milk used in this system may
508 be effective delivery systems for curcumin in functional food and beverage applications. It
509 should be noted that there are a number of limitations of the current study. We did not include
510 Phase I and II enzymes in our simulated gastrointestinal model, yet these are known to cause
511 extensive metabolism of curcumin within the human gut. In future studies, it will be important
512 to test the curcumin-loaded delivery systems using more realistic in vitro models or, better still,
513 using in vivo animal or human feeding studies. It will also be important to ensure that the

514 delivery systems can survive the harsh conditions that commercial foods and beverages
515 experience throughout their lifetime.

516 Acknowledgments

517 This material was partly based upon work supported by the National Institute of Food and
518 Agriculture, USDA, Massachusetts Agricultural Experiment Station (MAS00491) and USDA,
519 AFRI Grants (2016-08782).

520 References

521 1. M. U. Akbar, K. Rehman, K. M. Zia, M. I. Qadir, M. S. H. Akash and M. Ibrahim, Critical
522 Review on Curcumin as a Therapeutic Agent: From Traditional Herbal Medicine to an
523 Ideal Therapeutic Agent, *Critical Reviews in Eukaryotic Gene Expression*, 2018, **28**, 17-24.
524 2. H. Hatcher, R. Planalp, J. Cho, F. M. Tortia and S. V. Torti, Curcumin: From ancient medicine
525 to current clinical trials, *Cellular and Molecular Life Sciences*, 2008, **65**, 1631-1652.
526 3. T. Tsuda, Curcumin as a functional food-derived factor: degradation products, metabolites,
527 bioactivity, and future perspectives, *Food & Function*, 2018, **9**, 705-714.
528 4. J. Epstein, I. R. Sanderson and T. T. MacDonald, Curcumin as a therapeutic agent: the
529 evidence from in vitro, animal and human studies, *British Journal of Nutrition*, 2010, **103**,
530 1545-1557.
531 5. A. Kunwar and K. I. Priyadarsini, in *Anti-Inflammatory Nutraceuticals and Chronic Diseases*,
532 eds. S. C. Gupta, S. Prasad and B. B. Aggarwal, 2016, vol. 928, pp. 1-25.
533 6. H. Y. Zhou, C. S. Beevers and S. L. Huang, The Targets of Curcumin, *Current Drug Targets*,
534 2011, **12**, 332-347.
535 7. J. Higdon, V. J. Drake, B. Delage and L. Howells, Curcumin,
536 http://lpi.oregonstate.edu/mic/dietary-factors/phytochemicals/curcumin).
537 8. M. Heger, R. F. van Golen, M. Broekgaarden and M. C. Michel, The Molecular Basis for the
538 Pharmacokinetics and Pharmacodynamics of Curcumin and Its Metabolites in Relation
539 to Cancers, *Pharmacological Reviews*, 2014, **66**, 222-307.
540 9. Z. Stanic, Improving therapeutic effects of curcumin - a review, *Journal of Food and*
541 *Nutrition Research*, 2018, **57**, 109-129.
542 10. A. Araiza-Calahorra, M. Akhtar and A. Sarkar, Recent advances in emulsion-based delivery
543 approaches for curcumin: From encapsulation to bioaccessibility, *Trends in Food Science*
544 *& Technology*, 2018, **71**, 155-169.
545 11. P. A. Nayak, T. Mills and I. Norton, Lipid Based Nanosystems for Curcumin: Past, Present
546 and Future, *Current Pharmaceutical Design*, 2016, **22**, 4247-4256.

12. D. J. McClements, Nanoscale Nutrient Delivery Systems for Food Applications: Improving Bioactive Dispersibility, Stability, and Bioavailability, *Journal of Food Science*, 2015, **80**, N1602-N1611.
13. I. Krishnakumar, A. Ravi, D. Kumar, R. Kuttan and B. Maliakel, An enhanced bioavailable formulation of curcumin using fenugreek-derived soluble dietary fibre, *Journal of Functional Foods*, 2012, **4**, 348-357.
14. D. J. McClements, Delivery by Design (DbD): A Standardized Approach to the Development of Efficacious Nanoparticle- and Microparticle-Based Delivery Systems, *Comprehensive Reviews in Food Science and Food Safety*, 2018, **17**, 200-219.
15. K. Pan, Y. C. Luo, Y. D. Gan, S. J. Baek and Q. X. Zhong, pH-driven encapsulation of curcumin in self-assembled casein nanoparticles for enhanced dispersibility and bioactivity, *Soft Matter*, 2014, **10**, 6820-6830.
16. S. F. Peng, Z. L. Li, L. Q. Zou, W. Liu, C. M. Liu and D. J. McClements, Improving curcumin solubility and bioavailability by encapsulation in saponin-coated curcumin nanoparticles prepared using a simple pH-driven loading method, *Food & Function*, 2018, **9**, 1829-1839.
17. S. F. Peng, Z. L. Li, L. Q. Zou, W. Liu, C. M. Liu and D. J. McClements, Enhancement of Curcumin Bioavailability by Encapsulation in Sophorolipid-Coated Nanoparticles: An in Vitro and in Vivo Study, *Journal of Agricultural and Food Chemistry*, 2018, **66**, 1488-1497.
18. B. J. Zheng, S. F. Peng, X. Y. Zhang and D. J. McClements, Impact of Delivery System Type on Curcumin Bioaccessibility: Comparison of Curcumin-Loaded Nanoemulsions with Commercial Curcumin Supplements, *Journal of Agricultural and Food Chemistry*, 2018, **66**, 10816-10826.
19. Y. Li, M. Hu and D. J. McClements, Factors affecting lipase digestibility of emulsified lipids using an in vitro digestion model: proposal for a standardised pH-stat method, *Food Chemistry*, 2011, **126**, 498-505.
20. L. Zou, B. Zheng, R. Zhang, Z. Zhang, W. Liu, C. Liu, H. Xiao and D. J. McClements, Food-grade nanoparticles for encapsulation, protection and delivery of curcumin: comparison of lipid, protein, and phospholipid nanoparticles under simulated gastrointestinal conditions, *RSC Advances*, 2016, **6**, 3126-3136.
21. R. Zhang, Z. Zhang, H. Zhang, E. A. Decker and D. J. McClements, Influence of emulsifier type on gastrointestinal fate of oil-in-water emulsions containing anionic dietary fiber (pectin), *Food Hydrocolloids*, 2015, **45**, 175-185.
22. C. Cheng, S. Peng, Z. Li, L. Zou, W. Liu and C. Liu, Improved bioavailability of curcumin in liposomes prepared using a pH-driven, organic solvent-free, easily scalable process, *RSC Advances*, 2017, **7**, 25978-25986.
23. S. Peng, Z. Li, L. Zou, W. Liu, C. Liu and D. J. McClements, Enhancement of Curcumin Bioavailability by Encapsulation in Sophorolipid-Coated Nanoparticles: An in Vitro and in Vivo Study, *Journal of agricultural and food chemistry*, 2018, **66**, 1488-1497.
24. D. J. McClements, Colloidal basis of emulsion color, *Current opinion in colloid & interface science*, 2002, **7**, 451-455.
25. W. Chantrapornchai, F. M. Clydesdale and D. J. McClements, in *Color Quality of Fresh and Processed Foods*, eds. C. A. Culver and R. E. Wrolstad, American Chemical Society, Washington, D.C., 2008, vol. 983, pp. 364-387.

26. M. M. Robins, Emulsions—creaming phenomena, *Current opinion in colloid & interface science*, 2000, **5**, 265-272.
27. D. J. McClements, *Food Emulsions: Principles, Practices, and Techniques*, CRC Press, Boca Raton, FL, Third edn., 2015.
28. B. C. Chen, D. J. McClements, D. A. Gray and E. A. Decker, Stabilization of Soybean Oil Bodies by Enzyme (Laccase) Cross-Linking of Adsorbed Beet Pectin Coatings, *Journal of Agricultural and Food Chemistry*, 2010, **58**, 9259-9265.
29. D. Iwanaga, D. A. Gray, I. D. Fisk, E. A. Decker, J. Weiss and D. J. McClements, Extraction and characterization of oil bodies from soy beans: A natural source of pre-emulsified soybean oil, *Journal of Agricultural and Food Chemistry*, 2007, **55**, 8711-8716.
30. R. L. C. Chuang, J. C. F. Chen, J. Chu and J. T. C. Tzen, Characterization of seed oil bodies and their surface oleosin isoforms from rice embryos, *Journal of Biochemistry*, 1996, **120**, 74-81.
31. E. Silletti, M. H. Vingerhoeds, W. Norde and G. A. Van Aken, The role of electrostatics in saliva-induced emulsion flocculation, *Food Hydrocolloids*, 2007, **21**, 596-606.
32. M. H. Vingerhoeds, T. B. Blijdenstein, F. D. Zoet and G. A. van Aken, Emulsion flocculation induced by saliva and mucin, *Food Hydrocolloids*, 2005, **19**, 915-922.
33. Y. Chang and D. J. McClements, Characterization of mucin–lipid droplet interactions: Influence on potential fate of fish oil-in-water emulsions under simulated gastrointestinal conditions, *Food Hydrocolloids*, 2016, **56**, 425-433.
34. H. Singh, A. Ye and D. Horne, Structuring food emulsions in the gastrointestinal tract to modify lipid digestion, *Progress in lipid research*, 2009, **48**, 92-100.
35. N. Hettiarachchy and U. Kalapathy, Functional properties of soy proteins, 1998.
36. J. E. Kinsella, Functional properties of soy proteins, *Journal of the American Oil Chemists' Society*, 1979, **56**, 242-258.
37. B. Ozturk and D. J. McClements, Progress in natural emulsifiers for utilization in food emulsions, *Current Opinion in Food Science*, 2016, **7**, 1-6.
38. C. Chung, A. Sher, P. Rousset and D. J. McClements, Use of natural emulsifiers in model coffee creamers: Physical properties of quillaja saponin-stabilized emulsions, *Food hydrocolloids*, 2017, **67**, 111-119.
39. Y. Li and D. J. McClements, New mathematical model for interpreting pH-stat digestion profiles: Impact of lipid droplet characteristics on in vitro digestibility, *Journal of Agricultural and Food Chemistry*, 2010, **58**, 8085-8092.
40. L. Salvia-Trujillo, C. Qian, O. Martín-Belloso and D. McClements, Influence of particle size on lipid digestion and β-carotene bioaccessibility in emulsions and nanoemulsions, *Food chemistry*, 2013, **141**, 1472-1480.

Table 1.

	Control	Nanocrystals	Nanoemulsions	Oil Bodies
C_I (μg/mL)	250.00 ± 0 [a]	233.0± 7.2 [b]	233± 11 [b]	234.6± 9.0[b]
EE (%)	100 ± 0 [a]	93.2 ± 3.1 [b]	93.2 ± 4.8 [b]	94 ± 3.8 [b]
*L**	6.64 ±0.80 [a]	25.81 ± 0.24 [b]	84.41 ±0.17 [c]	82.41± 0.10 [c]
*a**	2.96 ± 0.74 [c]	-2.62 ± 0.13 [c]	-6.85 ± 0.06 [b]	-8.01 ± 0.09 [a]
*b**	7.2 ± 1.3 [a]	38.80 ± 0.75 [b]	80.5 ± 1.1 [c]	80.62 ± 0.48 [c]
ζ- potential (mV)	-	-	-55.8 ± 1.5 [a]	-30.3 ± 1.9 [b]
D_{32} (μm)	-	-	0.18 ± 0.02 [b]	0.41 ± 0.01 [a]

Table 1. The initial curcumin concentration (C_I), loading capacity, tristimulus color coordinates (*L*, a*, b**), mean particle diameter (D_{32}) and electrical characteristics (ζ- potential) of curcumin-loaded samples. Samples designated with different letters are significantly different (Duncan, $p < 0.05$).

Fig. 1a

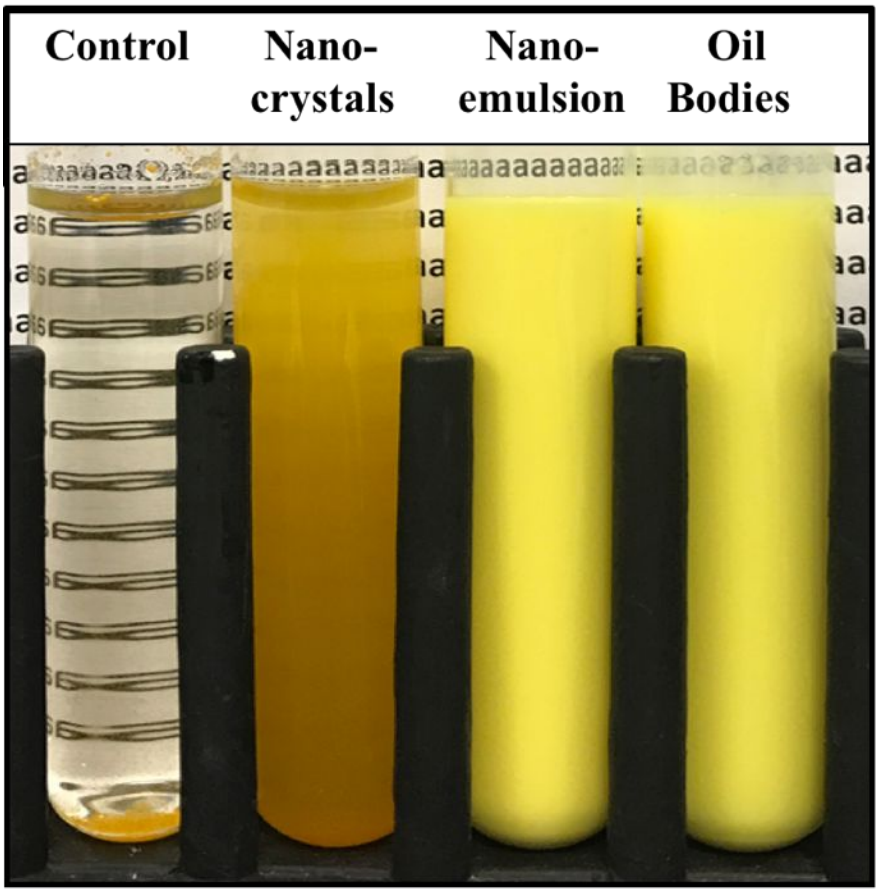

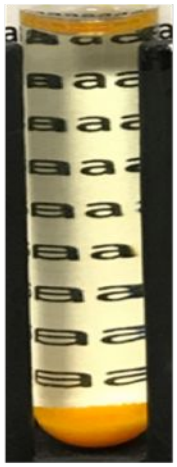

Nanocrystal 2-hour later

Fig.1 b:

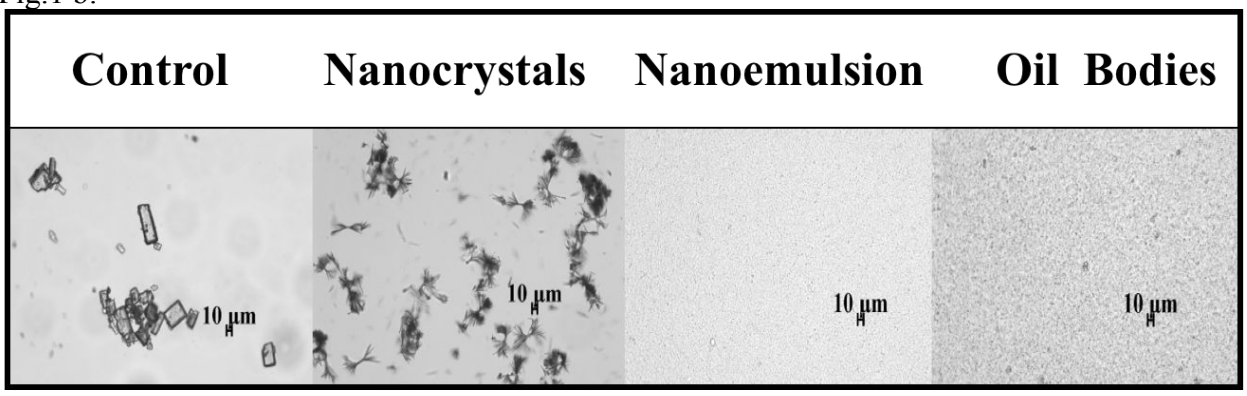

Fig. 1. (a) Appearances of curcumin containing sampes (right hand image shows nanocrystals after sedimentation). (b) light microscopy images of curcumin-containing samples. The small bars in the images represent a length of 10 μm.

Fig.2

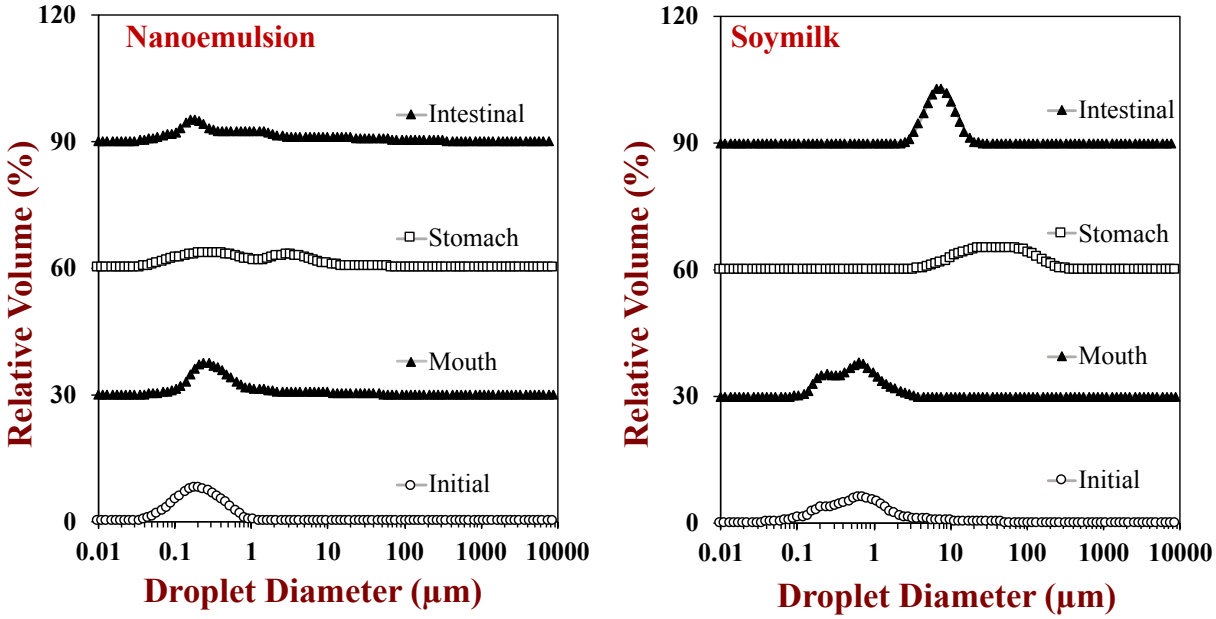

Fig. 2 Particle size distribution of curcumin-loaded emulsion and oil-bodies prepared using pH-driven method after undergo the different stages of a simulated gastrointestinal tract conditions.

Fig.3

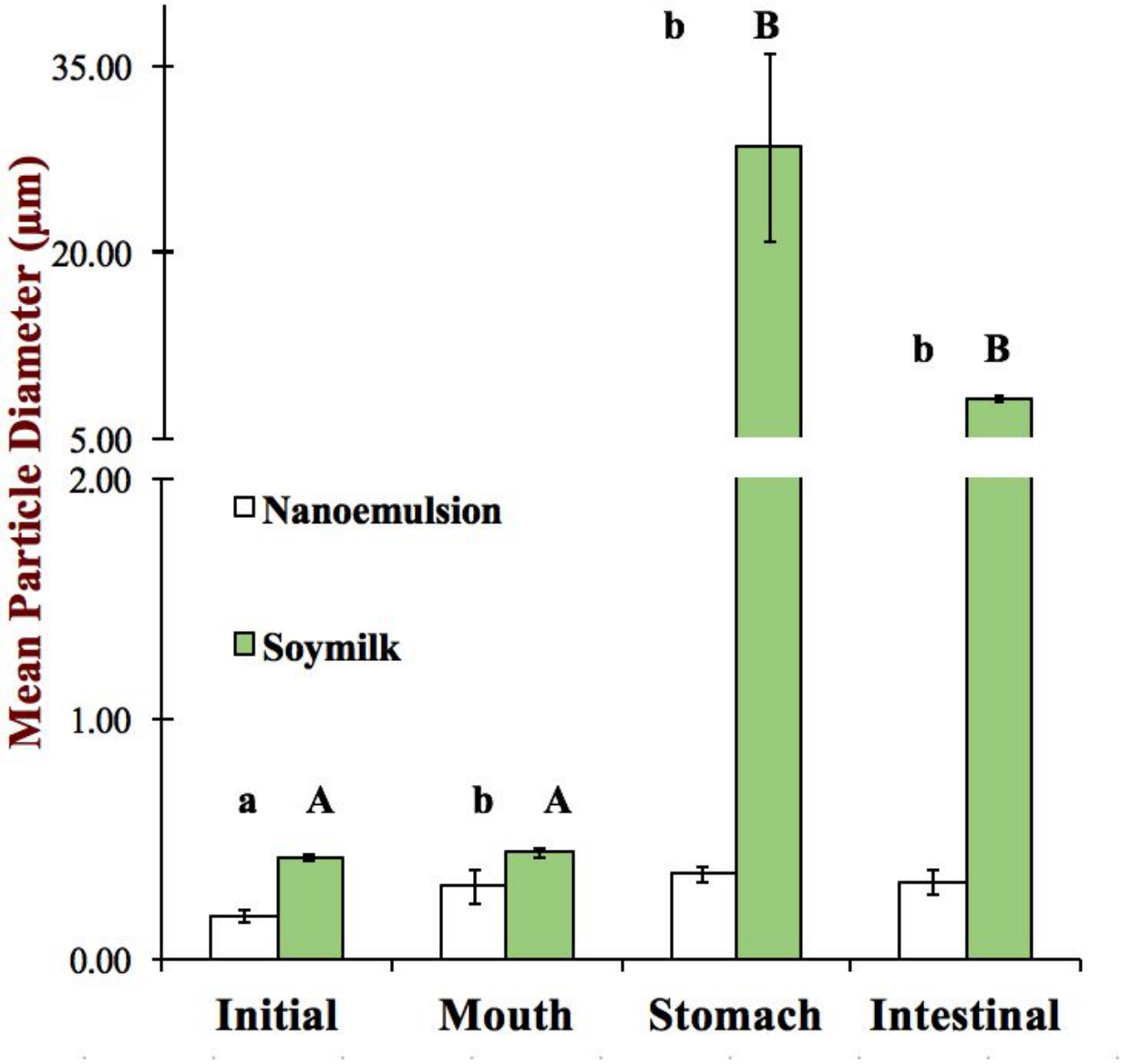

Fig.3 The Mean particle diameter (d_{32}) of the curcumin-loaded emulsion and oil-bodies under exposure to the simulated gastrointestinal tract model. Both Different lowercase and capital letters represent significant different (Duncan, $p < 0.05$) of the particle diameter between the same digestion phases

Fig.4

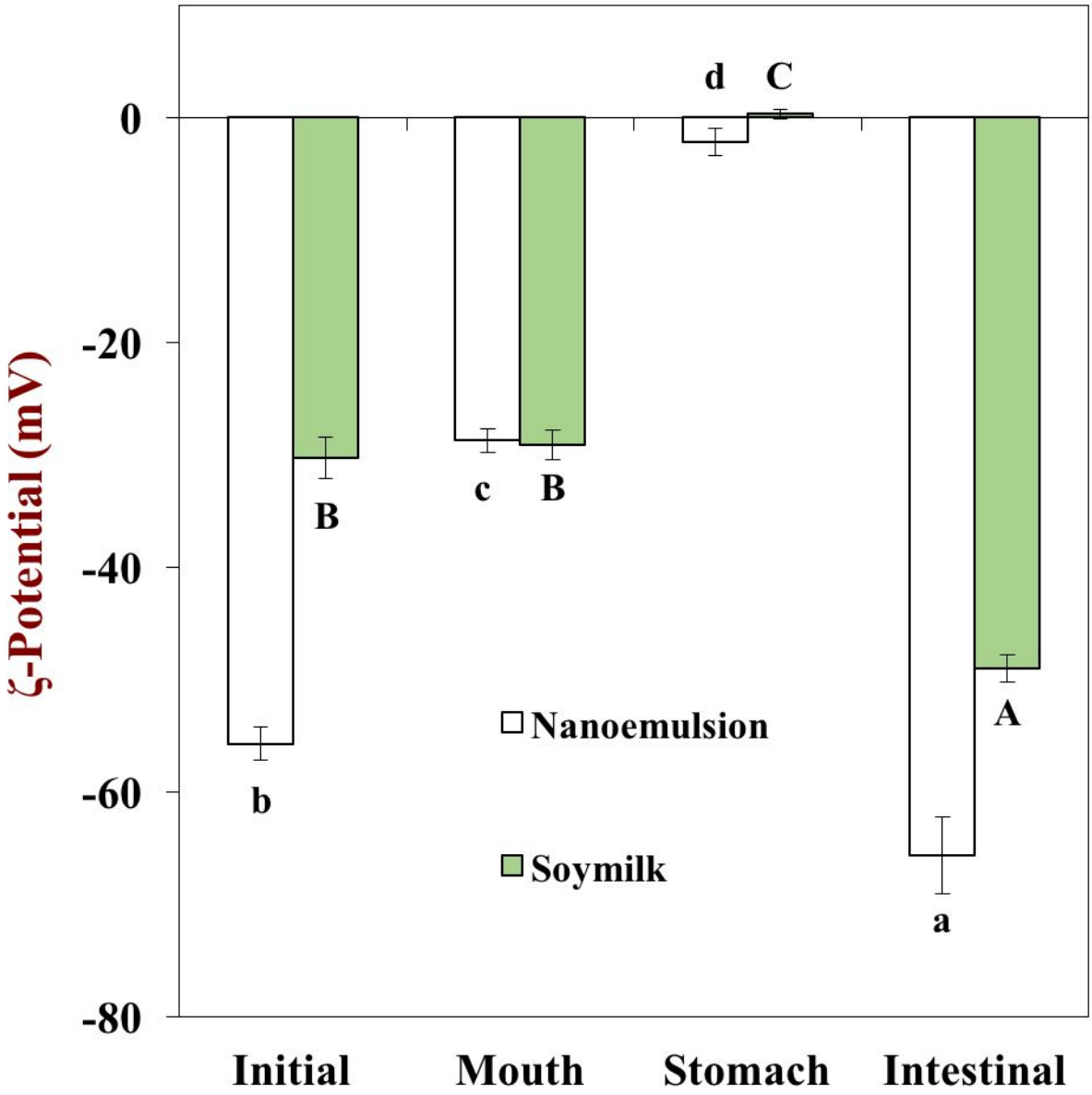

Fig. 4 influence of stimulated gastrointestinal tract models on the surface charge of the curcumin loaded nanoemulsion and oil-bodies. Both Different capital and lowercase letters mean significant difference (Duncan, $p < 0.05$) of the particle charge in samples between the same digestion phase;

Fig. 5

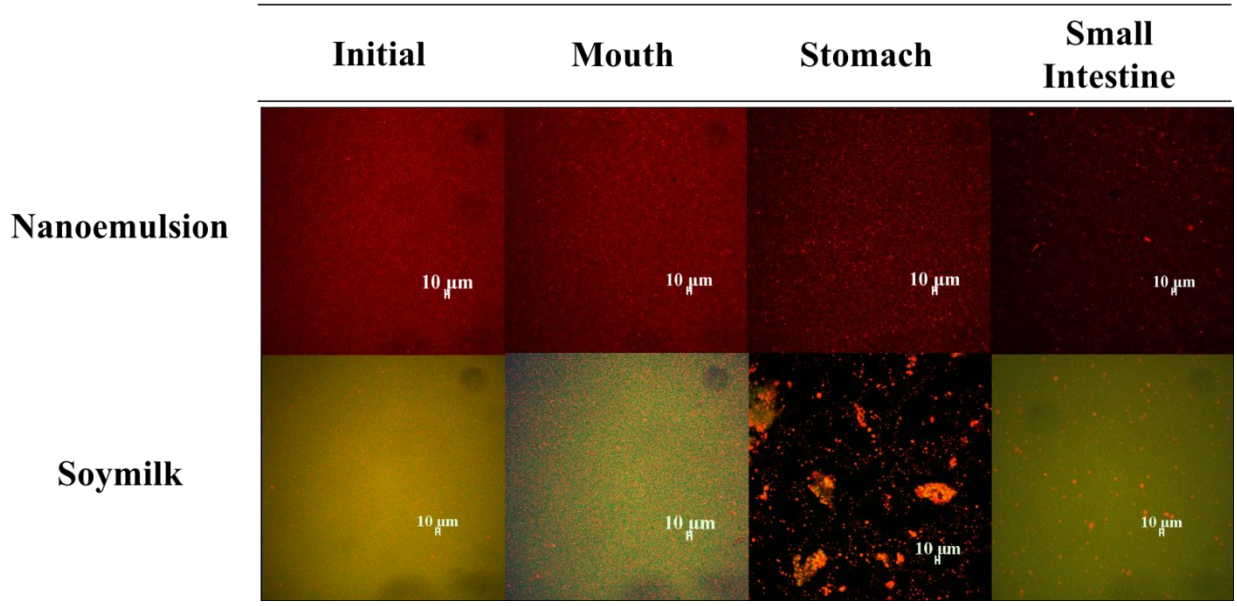

Fig. 5. The microstructure of the curcumin-loaded nanoemulsion and oil bodies under exposure to gastrointestinal condition. the confocal microscope was used to obtain the photo with fluorescent dye and a scale length of 10 μm. The red regions represent lipid and green means the protein

Fig. 6

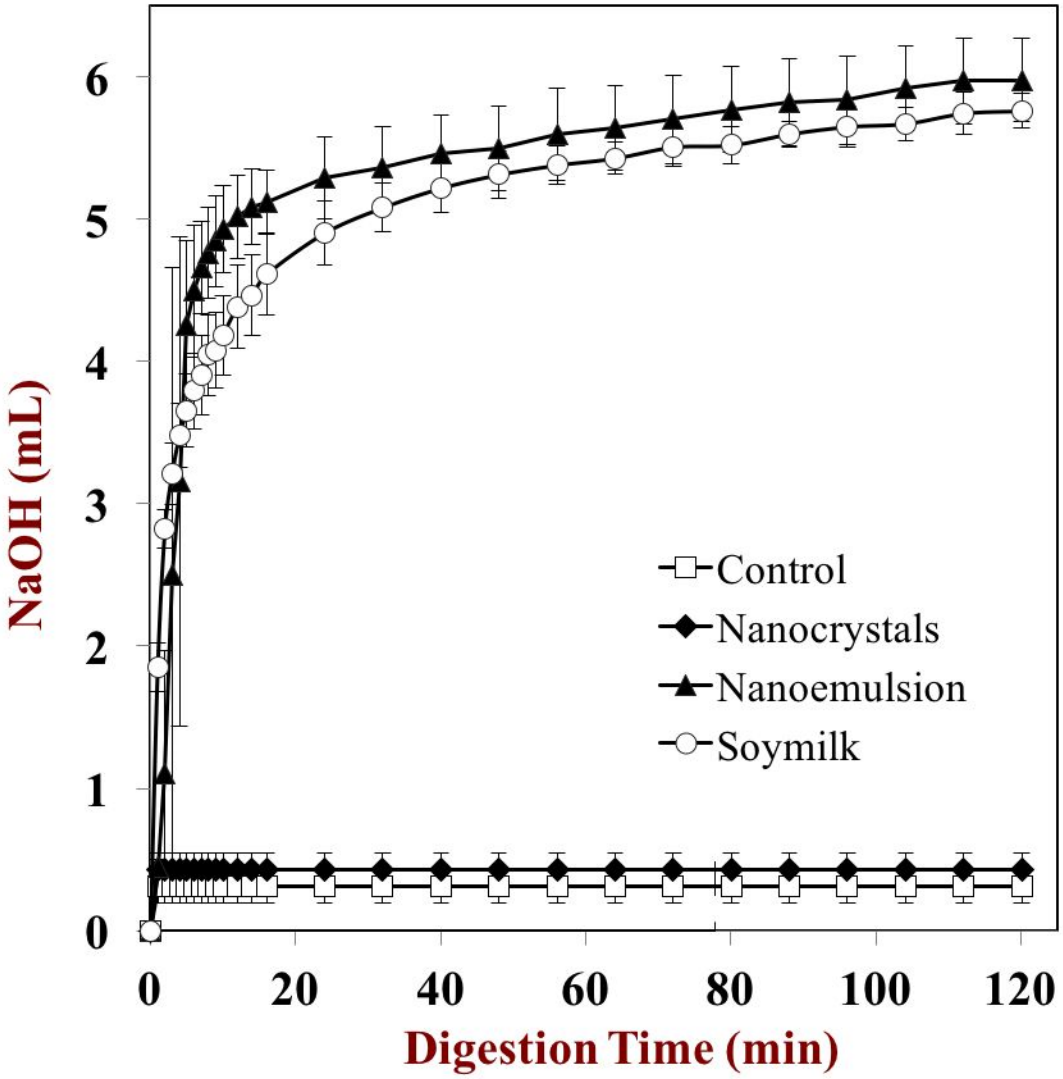

Fig. 6 a. The Calculated free fatty acid release profile for curcumin-loaded emulsion and oil bodies; b. influence of curcumin-loaded sample with and without lipid on NaOH profile

Fig. 7a

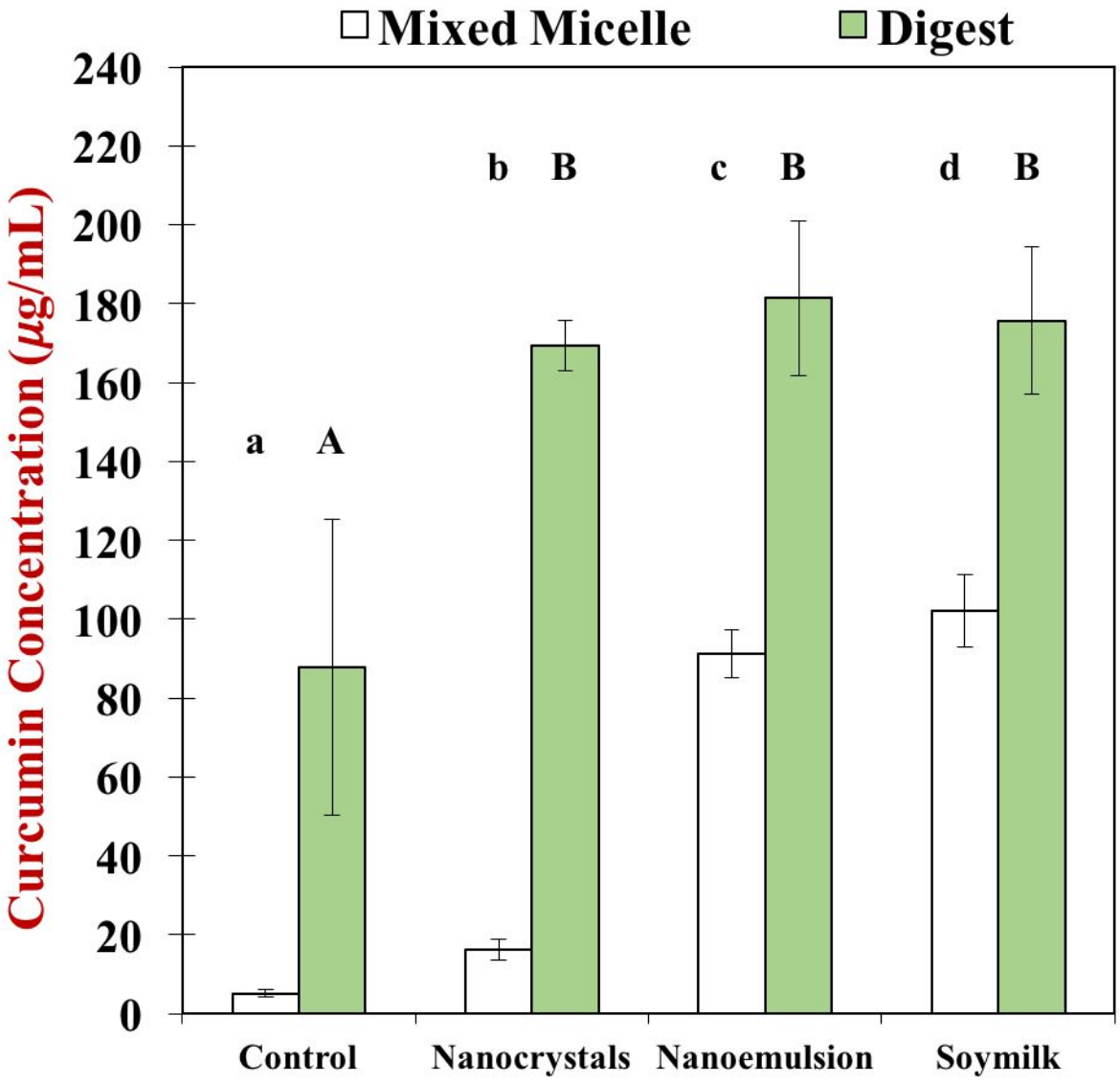
Mixed Micelle
Digest
Curcumin Concentration (μg/mL)
240
220
200
180
160
140
120
100
80
60
40
20
0
a A
b B
c B
d B
Control
Nanocrystals
Nanoemulsion
Soymilk

Fig. 7b

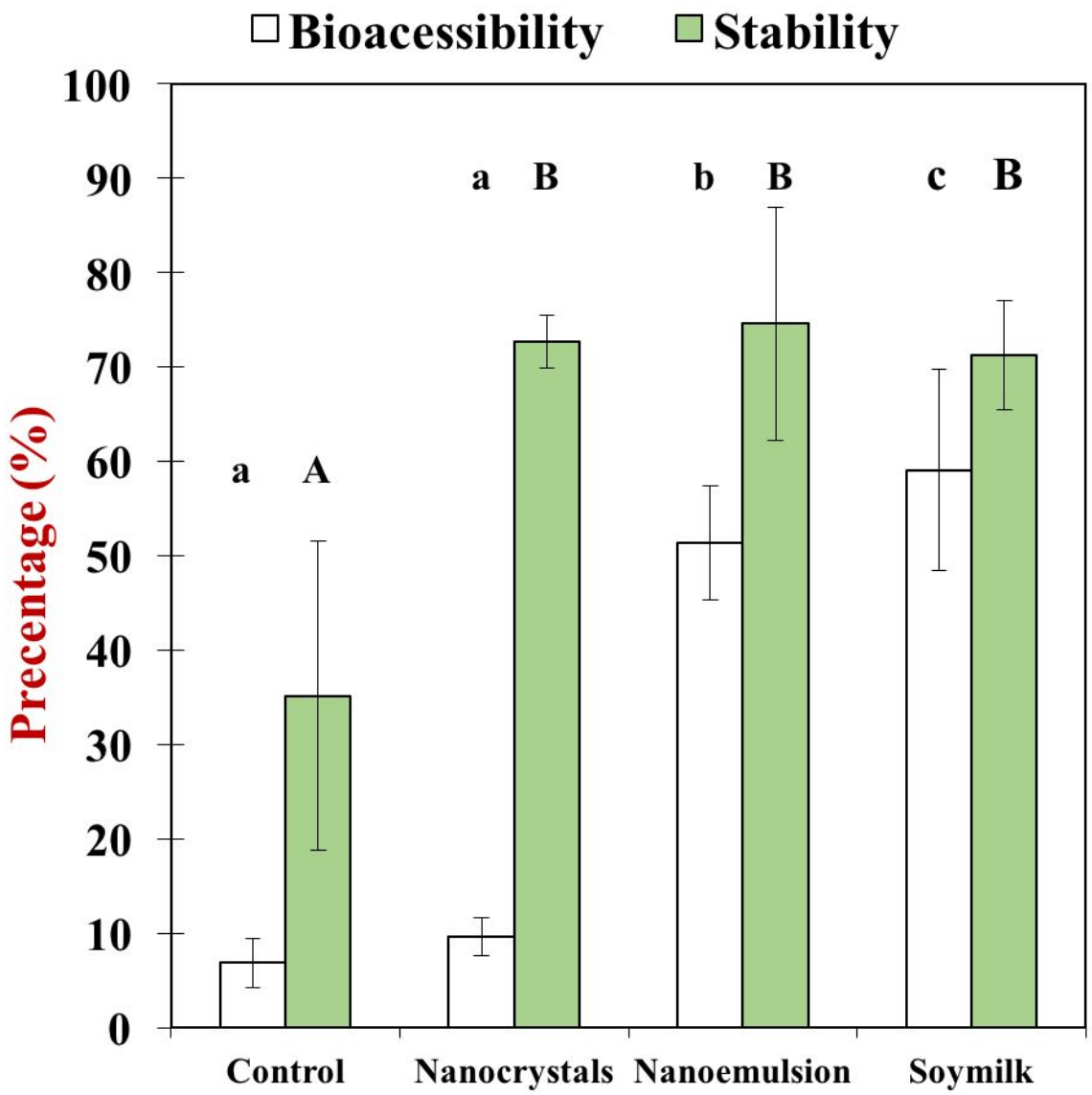

Fig 7 (a). Influence of curcumin-loaded water, emulsion and oil bodies on curcumin concentration in mixed micelles and raw digest; (b). and bioaccessibility and stability of curcumin. Different lowercase letters and capital letters both mean significant difference (Duncan, $p < 0.05$) of the particle charge in samples within the same digestion phases